Research Article
doi.org/10.1002/ansa.202100041
Chemistry Europe
European Chemical Societies Publishing

Received: 28 July 2021
Revised: 10 November 2021
Accepted: 15 November 2021

Synthesis, characterization, and comparative assessment of antimicrobial properties and cytotoxicity of graphene-, silver-, and zinc-based nanomaterials

Oindrila Hossain[1] | **Ehsanur Rahman**[1] | **Hridoy Roy**[1] | **Md. Shafiul Azam**[2] | **Shoeb Ahmed**[1]

[1] Department of Chemical Engineering, Bangladesh University of Engineering and Technology, Dhaka, Bangladesh

[2] Department of Chemistry, Bangladesh University of Engineering and Technology, Dhaka, Bangladesh

Correspondence
Shoeb Ahmed, Department of Chemical Engineering, Bangladesh University of Engineering and Technology, Dhaka, Bangladesh.
Email: shoebahmed@che.buet.ac.bd

Abstract

Zinc oxide (ZnO) and graphene oxide (GO) nanoparticles, silver/zinc zeolite (Ag/Zn-Ze), and graphene oxide-silver (GO-Ag) nanocomposites were synthesized and characterized with X-ray powder Diffraction, Field Emission Scanning Electron Microscope and Fourier Transform-Infrared Spectroscopy. The antibacterial efficacy of these nanoparticles was evaluated against *E. coli*. by shake flask method and plate culture method for different concentrations. For 10^5 cells/mL initial bacterial concentration, minimum inhibitory concentration (MIC) were <160, <320, <320, and >1280 μg/mL, and antibacterial concentration at which 50% cells are inhibited (IC_{50}) were 47, 90, 78, and 250 μg/mL for Ag/Zn-Ze, GO, GO-Ag, and ZnO, respectively. Therefore, the shake flask method showed that for all nanoparticle concentrations, Ag/Zn-Ze, and GO-Ag exhibited greater inhibition efficacy, which was also highly dependent on initial bacterial concentration. However, in case of the plate culture method, similar range of inhibition capacity was found for Ag/Zn-Ze, GO-Ag, and ZnO, whereas GO showed lower potency to inhibit *E. coli*. In addition, GO-Ag nanocomposite exhibited more efficacy than Ag/Zn-Ze when the antibacterial surface was prepared with those. However, Ag/Zn-Ze showed no toxicity on Vero cells, whereas GO-Ag exhibited severe toxicity at higher concentrations. This study establishes GO-Ag and Ag/Zn-Ze as potent antimicrobial agents; however, their application dosage should carefully be chosen based on cytotoxic effects of GO-Ag in case of any possible physiological interaction.

KEYWORDS
antibacterial agent, cytotoxicity, graphene oxide, nanocomposites

Research Article
doi.org/10.1002/ansa.202100041
Chemistry Europe
European Chemical Societies Publishing

1 | INTRODUCTION

Microorganisms like pathogenic bacteria, protozoan parasites, and fungi are known to trigger many infectious diseases. The emergence of infectious diseases is increasing rapidly, and they are becoming drug resistant.[1] Some of the present developing infections are not new, and they were reported to be fatal before. Though there is increased knowledge of microbial pathogenesis and application of modern therapeutics, the morbidity and mortality associated with the microbial infections remain high.[2] It is estimated that approximately 48 million cases of pathogenic diseases occurred in the United States in 2010.[3] Therefore, it is crucial to keep the pathogenic microbial contamination under control. To control emerging and re-emerging bacterial diseases, new antimicrobial agents are needed to discover from natural and inorganic substances.

Generally, antibacterial agents can be of two types, organic and inorganic antibacterial agents. Organic antibacterial materials are often less stable, particularly at high temperatures and/or pressures compared to inorganic antibacterial agents.[4] Consequently, inorganic single and composite materials have attracted lots of attention over the past decade due to their ability to withstand harsh process conditions.[5–9] These antimicrobial agents are believed to cause the disruption of bacterial membranes and the hindrance of biofilm formation.[10]

Because of the resistance problem, a renewed effort is to be made to seek antibacterial agents effective against pathogenic bacteria resistant to current antibacterials.[1] Hence, it is important to discover newer strategies and identify novel antimicrobial agents from natural and inorganic substances to develop next-generation solutions to manage microbial infections. Silver and copper, the two most widely used elements, had been used for this purpose since ancient times prior to the current applications as chemotherapeutics in modern health care systems.[11] In recent times, with the advancements in nanoscience and nanotechnology, nanosized inorganic and organic particles have captured the attention of researchers. These nanosized materials are being used in increasing applications as amendments in industrial, medicine and therapeutics, synthetic textiles, and food packaging products.[12]

Some of the inorganic antibacterial materials, in particular, some single nanoparticles such as TiO_2, ZnO, SnO_2, MgO, CaO, Mn_3O_4, Fe_3O_4, Ag, Au, GO have been suggested to have antimicrobial properties.[4,13–17] Composites from two or more of such particles might also be promising in case of possible synergistic effect.[18] Though there are many studies on nanomaterials, the majority of them only investigated whether the material works as an antibacterial agent or not.[17,19,20] However, it is also necessary to investigate their cytotoxicity, which is a prerequisite for using these materials in real life. Also, utilizing these nanomaterials to prepare the antibacterial surface and evaluation of their antimicrobial efficacy are crucial as typically, these materials will not be used in powdered form for real-life applications. To better understand these aspects, this study has been designed where an intensive experimental study has been conducted to develop a bridge between the existing research findings and current needs. Here, ZnO, GO GO-Ag, and Ag/Zn-Ze have been selected and their antimicrobial efficacies were evaluated against *E.Coli* in terms of Minimum Bactericidal Concentration (MBC), Minimum Inhibitory Concentration (MIC), and Half Maximal Inhibitory Concentration (IC_{50}) values. Two nanomaterials were further studied to prepare antibacterial surfaces. Also, the cytotoxicity of these two materials is studied as higher cytotoxicity could limit their applications. The nontoxic antibacterial agents can be used as a drug in the future to control microbial diseases. Here, ZnO and GO were selected as they are among the most studied nanomaterials. Au was excluded because of its high price. Ag and TiO_2 were not chosen for this research because of their higher cytotoxic effect.[13,21] GO-Ag was selected to achieve a synergistic effect. Moreover, Ag/Zn-Ze was selected because it is expected to give a synergistic effect, and the material is cheaper than GO-Ag. As the antibacterial activities of these nanomaterials are reported previously, our goal is to push forward the efforts for using these materials for practical applications. To accomplish our goal, two nanomaterials among these four were considered to prepare and evaluate the antibacterial surfaces based on their antibacterial activities.

2 | METHODOLOGY

2.1 | Preparation of nanoparticles

2.1.1 | ZnO

The ZnO nanoparticles were prepared by the precipitation method using zinc nitrate and sodium hydroxide as precursors and soluble starch as a stabilizing agent.[22] Note that 0.3 g of starch, dissolved in 100 mL of distilled water, was mixed with 10 mL 0.1 M zinc nitrate. The solution was stirred for 2 h until the complete dissolution occurred. 10 mL 0.2 M sodium hydroxide solution was added drop by drop to the above mixture, and the mixing was allowed to proceed for 2 h afterward. The reacted solution was allowed to settle down for 24 h. The bottom solution was centrifuged to obtain the precipitate. In order to remove the byproducts and excessive starch bound to the nanoparticles, the precipitate was washed with ethanol repeatedly. The powder of the ZnO nanoparticles was obtained after drying at 100°C for 2 h.

2.1.2 | Ag/Zn loaded zeolite

The antibacterial modified zeolite was prepared according to the method described earlier by Hacer Dogan et al.[23] Briefly, 50 g of zeolite clinoptilolite powder was oven-dried at 105°C for 1 h, and mixed with 50 g of distilled water. To adjust the pH between mild acidic to neutral region (= 5 to 7), 95 mL 0.5 N nitric acid solution was added to the solution. Then, the prepared slurry of zeolite clinoptilolite was put into contact with 0.1 M zinc nitrate and 0.4 M silver nitrate solutions. The liquid/solid ratio of the solution was kept as 5:1 (w/w), and the slurry was stirred at 50°C for 5 h to achieve significant ion exchange. The slurry

Research Article
doi.org/10.1002/ansa.202100041
Chemistry Europe
European Chemical Societies Publishing

was washed several times with distilled water by centrifugation, dried at 110°C for 5 h, and crushed into powder form.[23]

2.1.3 | GO

Oxidized graphene powders were synthesized according to the modified Hummers method.[24] Two grams of graphite was put into an 80°C solution of concentrated H_2SO_4 (12 mL) and HNO_3 (8 mL). The mixture was kept at 80°C for 8 h using an oil-bath. After cooling to room temperature, the mixture was diluted with 0.5 L of de-ionized (DI) water and left overnight. The mixture was filtered and washed with DI water using a vacuum pump filtration system to remove the residual acid. The product was dried under ambient conditions overnight. Pre-oxidized graphite powder (1 g), $NaNO_3$ (1.03 g), and concentrated H_2SO_4 (62 g) were placed in a flask, and 4.5 g of $KMnO_4$ was slowly added under stirring at 20°C for 2 h. After further vigorous stirring for 2 days at room temperature, the reaction was terminated by adding DI water (140 mL) and 30% H_2O_2 solution (2.5 mL). The mixture was filtered and washed by repeated centrifugation and filtration using 1 M HCl and DI water. The obtained mixture was dialyzed through semipermeable membranes for one week to remove the remaining metal species and was dried at 50°C to obtain the final product.

2.1.4 | GO-Ag nanocomposites

GO-Ag composite was prepared by the reduction of $AgNO_3$ using sodium borohydride in the presence of GO dispersion. As synthesized 3 mg GO powder was initially dispersed in 100 mL of distilled water, then 60 mg of $AgNO_3$ salt was added into the dispersion. The dispersion was then boiled, followed by rapid addition of 22 mg of sodium borohydride, and it was further boiled for 2 h. Finally, the GO—Ag nanohybrids were centrifuged at 20000 rpm for 20 min, washed several times with distilled water to remove unreacted reagents, and dried at 50°C under vacuum for 12 h.[25]

2.2 | Characterization techniques of antibacterial agents

FTIR spectra of ZnO, Ag/Zn loaded zeolite, GO, and GO-Ag were recorded in the range of 4000-400 cm^{-1} in transmission mode using an FTIR-8400 (Shimadzu, Japan). Before analysis, the samples were sonicated in water, oven-dried, and then mixed with crushed KBr powder (spectral grade, Sigma-Aldrich, Germany) and pressed to form pellets for the analysis. Morphological images of the prepared materials were recorded using a field emission scanning electron microscope (FESEM), JSM-7600F (JEOL, Japan) at a 10.0 kV operating voltage. A drop of a dilute aqueous suspension of the samples was taken in a glass plate and vacuum dried, and the surface was coated with a thin layer of gold. X-ray diffraction (XRD) patterns of the oven-dried samples were recorded using an X-ray diffractometer (RIGAKU Ultima IV, X-ray Diffractometer, Japan), with a Cu X-ray source (wavelength: Kα1 = 1.540598 Å and Kα2 = 1.544426 Å) in the 10 to 50° 2θ range. Before analysis, the samples were sonicated in water and oven-dried for 24 h at 50°C.

2.3 | Determination of antimicrobial activity

Antimicrobial activity of ZnO, Ag/Zn loaded zeolite, GO, and GO-Ag was evaluated against *E. coli* by both the shake flask method and zone of inhibition method. An individual colony of *E. coli* was picked up from a previously prepared culture plate and was aseptically transferred into 50 mL of sterile nutrient broth inside biosafety hood (LabTech, Korea). The solution was incubated, and the number of cells was determined based on optical density at 600 nm (OD_{600}). The microorganisms (10^7 and 10^5 cells/mL) were incubated with seven different concentrations of ZnO nanoparticles, Ag/Zn Zeolite nanocomposites, GO nanoparticles, and GO-Ag nanocomposites in nutrient broth at 200 rpm (Shaker: Phoenix Instrument, Germany) and 37°C for 3 h. Negative control was also prepared without any antimicrobial agents. After incubation, the optical density (OD_{600}) of the cell solutions was measured in a spectrophotometer (Hach DR6000, USA). The loss of cell viability (%) was determined based on the number of cells grown in the negative control.

Microorganisms were streaked over the surface of the MHAB culture plate, where antibacterial agents (50-100 μL) were poured into the artificially created wells. The plates were incubated at 37°C for 18-24 h, and the antibacterial activity was measured based on the thickness of the inhibition zone.

To evaluate the antibacterial property of a surface coated with the antibacterial nanocomposites, small pieces of filter paper were incubated overnight in the antibacterial nanoparticle solution in a shaker incubator. The nanoparticle-coated paper was dried and was used to cover the conical flasks filled with nutrient broth solution. The broth-containing flasks were kept outside of the biosafety hood for 24 h before measuring OD_{600}.

2.4 | Cytotoxicity test of antibacterial agents

Vero cells (15×10^4 cells per mL) were seeded into 96-well plate and incubated at 37°C, 5% CO_2 for 24 h. Growth media was replaced with 80 μL fresh media (DMEM) as well as 20 μL of solution of antibacterial agents. Then cytotoxicity was examined after 24 hours using CellTiter 96 Non-Radioactive Cell Proliferation Assay kit (Promega, USA).

3 | RESULTS AND DISCUSSION

3.1 | Characterization of prepared antibacterial agents

FTIR spectrum (shown in Figure 1) revealed the characteristic bonds of the prepared composites. The successful oxidation of graphene sheets

Research Article
doi.org/10.1002/ansa.202100041
Chemistry Europe
European Chemical Societies Publishing

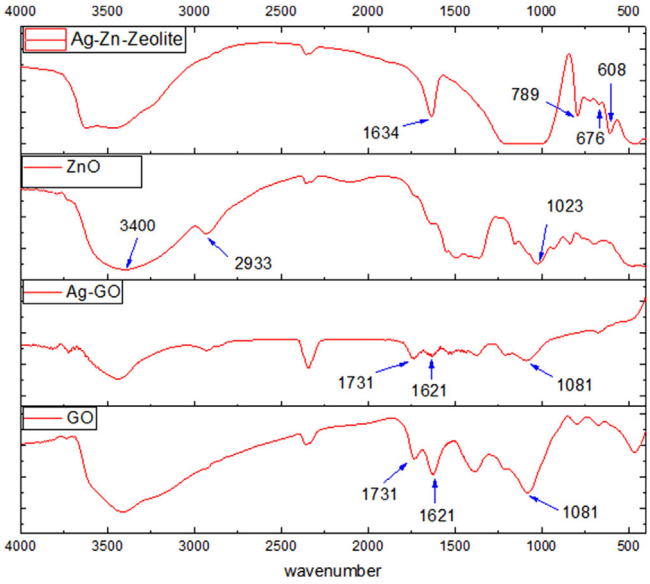

FIGURE 1 FTIR spectra of GO, GO-Ag, ZnO, Ag-Zn/Zeolite

can be confirmed by the peak at 1081 cm^{-1}, which attributes to the stretching of the C-O bond of GO samples.[26] Also, the peaks near 1621, 1731, and broad 3300-3500 cm^{-1} confirm the presence of C = C, C = O, and O-H bonds, respectively.[27] All the characteristic peaks of GO are found in GO-Ag nanocomposite, but the decrease in the intensity of C-O, C = O, and O-H bonds happened due to the incorporation of Ag nanoparticles and partial reduction of GO sheets.[28,29] The absorption peak at 3400 cm^{-1} of the ZnO sample is assigned to the stretching of O-H bonds of ZnOH, while the peaks at 1023 and 2933 cm^{-1} correspond to the C-O and C-H vibrations of the residual starch sample, respectively.[30] In the spectrum of Ag/Zn-Zeolite, the peaks between 461-969 cm^{-1} are assigned to the vibrations of Si-O, while Al-O bond is confirmed by the peak at 676 cm^{-1}.[31] Also, the peaks at 1634 and 3453 cm^{-1} appear due to the O-H bonds of adsorbed moisture.[31]

To explore the morphology and composition of the antibacterial nanomaterials, FESEM and EDS studies have been done. The results from these characterization techniques are portrayed in Figure 2. The FESEM image of ZnO nanoparticles confirmed that the particles are rod-shaped and highly agglomerated (Figure 2a). 13.27% carbon in the EDS result of ZnO nanoparticles indicates the presence of unwashed starch. As seen from the FESEM image of Ag/Zn-Ze nanocomposites (Figure 2b), the particles are rod-shaped, and the diameters of the rods are around 80-100 nm. It is well known that GO is often in the form of exfoliated sheet.[32] FESEM image of GO nanoparticles (Figure 2c) exhibited similar morphology. Figure 2d shows that the spherical Ag particles are embedded on the GO sheet where the diameter of the Ag particles is around 20-60 nm. Also, the EDS result confirms the existence of Ag nanoparticles on the GO surface.

Figure 3 illustrates the findings from XRD, which have been done to get an idea about the crystalline structures of the nanomaterials. The ZnO nanoparticles were observed to be crystalline, and a similar type of peak was found in the literature.[22] The XRD peaks are broad due to the nano-size effect. The average crystallite size of prepared ZnO nanoparticles was calculated using Scherrer's relation

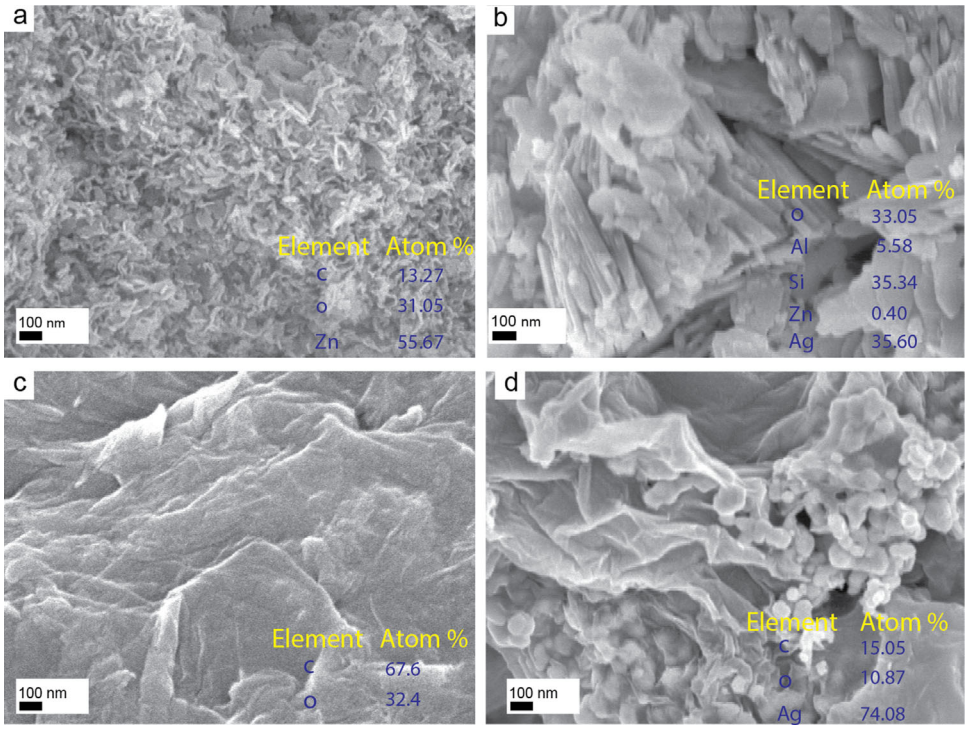

FIGURE 2 FESEM images of (a) ZnO (b) Ag-Zn/Zeolite (c) GO, and (d) GO-Ag. The inset tables represent the atomic compositions of the corresponding materials

Research Article
doi.org/10.1002/ansa.202100041
Chemistry Europe
European Chemical Societies Publishing

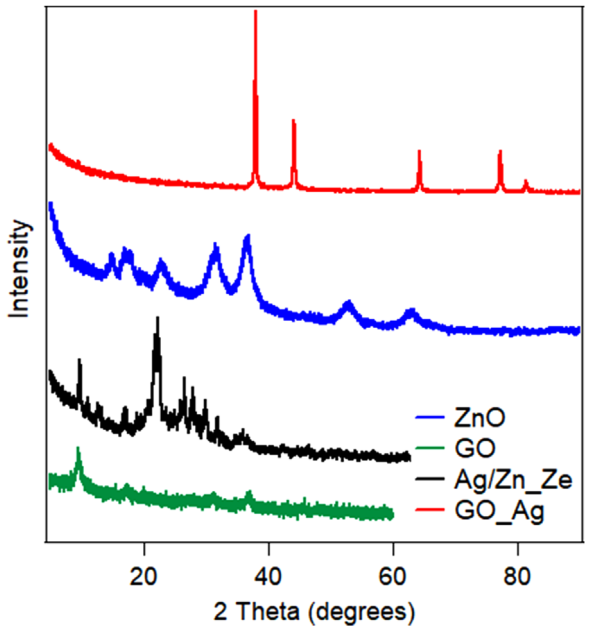

FIGURE 3 XRD imaging of ZnO nanoparticles, Ag/Zn-Ze nanocomposites, GO nanoparticles and GO-Ag nanocomposites

is about 20.77 nm. As seen from the XRD pattern, Ag/Zn-Ze composite was highly crystalline, and the average crystallite size of Ag/Zn-Ze nanocomposites was found to be 18 nm. The XRD pattern of GO nanoparticles shows a diffraction peak at $2\theta = 9.4^{o,}$ which confirms the formation of graphene oxide.[33] The corresponding interlayer spacing is measured as 0.93 nm via Bragg's equation, and it was similar to previous studies.[33] The interlayer spacing of GO is usually higher than graphite and is caused by loosely stacked GO.[34] The presence of many oxygen-based groups makes the interlayer spacing big.[35] The complete disappearance of the graphitic peak at $2\theta = 34^{o}$ ensures that the product is completely oxidized. The average crystal size of GO nanoparticles was 14 nm. The XRD curve of GO-Ag nanocomposites showed characteristic peaks at 2θ values of about 37.5°, 44°, and 64.1°. These values are related to the planes (1 1 1), (2 0 0), and (2 2 0) of silver crystal structure. The formation of silver crystal nanoparticles on the surface of GO sheet has been confirmed by these peaks.[25] The average crystal size of GO-Ag nanocomposites was 25 nm.

3.2 | Antibacterial activity test

The antibacterial properties of ZnO, Ag/Zn-Ze, GO, and GO-Ag were assessed through two different methods.

3.2.1 | Shake flask method

Using shake flask technique, OD_{600} values, number of viable cells, percentage of viable cells, and percentage removal of cells were obtained for studied antibacterial agents for 3 hrs incubation period. For two initial bacterial concentrations (10^5 and 10^7 cells/mL), optical density at 600 nm, OD_{600} values were taken at different concentrations of antibacterial compounds. The number of viable cells is proportional to the values of OD_{600}. As expected, for each case, after a three hours incubation period, the number of cells was greater for higher initial concentration of bacteria (10^7 cells/mL) compared to those for lower initial concentration of bacteria (10^5 cells/mL) (Figure 4). Similar phenomena were observed when percentage of viable cells were plotted (Figure 5).

viability

In the case of both bacterial concentrations, percentage removal increased with the increasing concentrations of ZnO nanoparticles (Figure 5a,b). For ZnO concentration of 20-80 μg/mL, no inhibition was exhibited. Table S1 shows the details of average OD_{600} values, average number of viable cells per mL, percentage of viable cells, and percentage removal of cells in the presence of ZnO nanoparticles. Here, the effectiveness was only marginally higher for lower initial cell concentration. 95% and 85% bacteria removal were achieved for lower and higher initial cell concentrations, respectively. However, 1280 μg/mL ZnO was unable to remove the bacteria completely even for lower initial cell concentration. Several previous studies of antibacterial efficiency of ZnO against *E. coli* bacteria have also shown that ZnO rarely removed bacteria cells completely.[36]

Table S2 shows the details of average OD_{600} values, average number of viable cells per mL, percentage of viable cells, and percentage removal of cells in the presence of Ag/Zn-Ze nanocomposite. From Figure 5a, b, it was found that the trend of cell viability was similar to ZnO nanoparticles for both initial bacterial concentrations; however, the

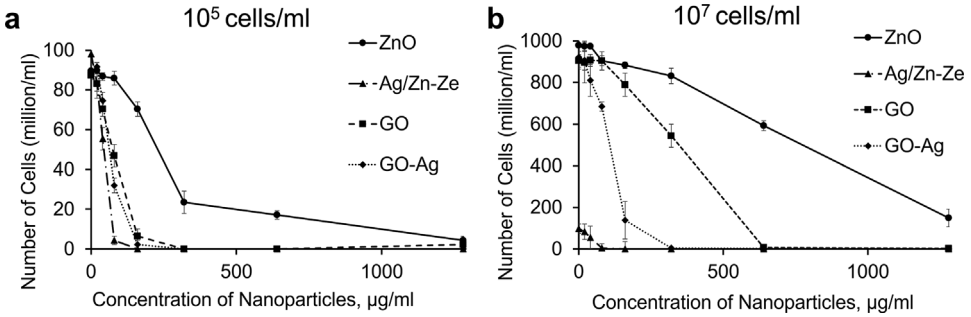

FIGURE 4 Number of *E. coli*. cells in different concentration of antibacterial agents (a) initial bacterial concentration 10^5 cells/mL (b) initial bacterial concentration 10^7 cells/mL. Error bars indicate the standard error of three or more independent experiments

Research Article
doi.org/10.1002/ansa.202100041
Chemistry Europe
European Chemical Societies Publishing

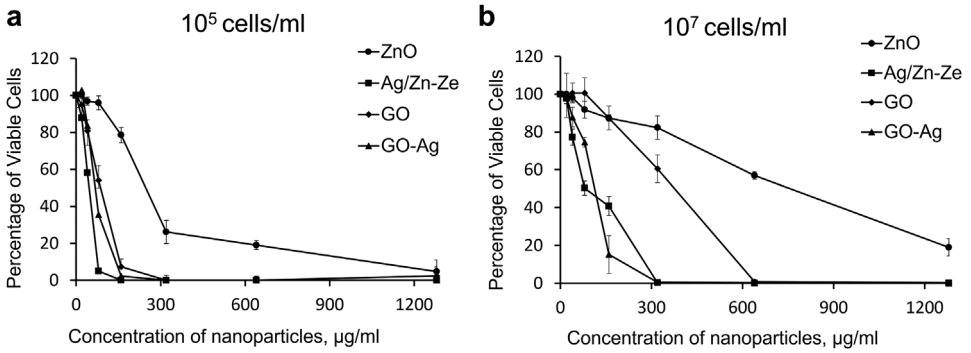

FIGURE 5 Percentage of viable *E. coli* cells for different concentration of antibacterial agents (a) initial bacterial concentration 10^5 cells/mL (b) initial bacterial concentration 10^7 cells/mL. Error bars indicate the standard error of three or more independent experiments

values reached zero for a significantly lower concentration of Ag/Zn-Ze compared to ZnO, indicating its more potent antibacterial efficacy. *E. coli* was removed entirely at 160 μg/mL and 320 μg/mL in case of low and high initial cell concentrations, respectively.

As seen from Figures 4 and 5, GO was also able to remove all the bacterial cells for both initial concentration scenarios. Cells were completely removed at 320 μg/mL and 1280 μg/mL in case of low and high initial cell concentrations, respectively. GO-Ag proved to be very effective in removing *E. coli* bacteria (Figures 4 and 5). Even at low concentrations (320 μg/mL) of GO-Ag, almost complete removal of bacteria was achieved when the initial cell concentration was higher. This is consistent with the previous study of antibacterial efficiency of GO-Ag and GO against *E. coli* bacteria.[37] Table S3 and S4 show the details of average OD_{600} values, average number of viable cells per mL, percentage of viable cells, and percentage removal of cells for GO and GO-Ag nanocomposite, respectively.

MIC and IC_{50}

Half-maximal inhibitory concentration (IC_{50}) was calculated from Figure 5. The effect of ZnO is also found from Figure 5 as 250 μg/mL and 785 μg/mL for low and high initial cell concentration scenarios, respectively. The effect of initial cell concentration on the effectiveness of the antibacterial compounds is discernable from the result. MIC for ZnO was higher than 1280 μg/mL for both cell concentrations. It has been reported that the MIC for ZnO can be up to 3100 μg /mL for *E. coli*.[38] Consistent with this study, the efficacy of ZnO nanoparticles was found to be dependent on the initial bacterial concentration as with the increase of initial bacterial concentration, it cannot prohibit the growth of *E. coli*. completely.[36]

As discussed before, Ag/Zn-Ze was very effective and was able to remove cells completely at a relatively low concentration. MIC was found to be 160 μg/mL and 320 μg/mL for low and high initial cell concentrations, respectively. Accordingly, IC_{50} values were also significantly low (47 μg/mL and 83 μg/mL for low and high initial cell concentration scenario, respectively).

Previous studies of antibacterial efficiency of GO against *E. coli* bacteria indicated that GO could fully remove bacteria.[33] MIC was found to be 320 μg/mL and 1280 μg/mL for low and high initial cell concentrations, respectively. IC_{50} values were 90 μg/mL and 370 μg/mL for low and high initial cell concentrations, respectively (Figure 5). GO-Ag exhibited potent inhibition as the IC_{50} values were 78 μg/mL and 113 μg/mL for low and high initial cell concentrations, respectively (Figure 5). MIC for both cases was 320 μg/mL, which is consistent with the previous report that GO-Ag might removes cells completely at 100-1000 μg/mL concentration depending on initial bacterial concentration.[33,37] Although both Ag/Zn-Ze and GO-Ag exhibited the same antibacterial efficacy in complete cell removal, Ag/Zn-Ze was found to be more effective in IC_{50}.

Comparison of antibacterial agents

Table S5 shows the percentage of viable cells of *E. coli*. bacteria after 3 hrs of incubation with different antibacterial agents at different concentrations in case of 10^5 cells/mL initial cell concentration. The activity of Ag/Zn-Ze was better than the other three agents as it fully inhibited the growth of bacteria at 160 μg/mL concentration, whereas these values are 320 μg/mL and 320 μg/mL for GO and GO-Ag, respectively. ZnO was not able to inhibit completely at 1280 μg/mL concentration. Table S6 presents similar data for the high initial cell concentration (10^7 cells/mL). Here, the activity of Ag/Zn-Ze and GO-Ag was better than the other two agents. At higher initial cell concentration, the activity of ZnO was found low.

As seen from Figure 6, at lower concentration antibacterial compounds such as 20 μg/mL, the activities of all compounds were more or less the same for higher initial bacterial concentration. At lower initial bacterial concentration Ag/Zn-Ze performed better than other compounds. At higher bacterial concentration GO-Ag showed greater inhibitory capacity than ZnO and GO. Tang et al. and Chandraker et al. studied the effect of GO-Ag nanoparticles on various bacteria and found that GO-Ag has a tremendous effect on inhibiting *E. coli* growth.[39,40] However, Ag/Zn-Ze exhibited the best performance among studied antibacterial compounds. At intermediate concentrations (80 and 160 μg/mL), the antibacterial performances of ZnO, GO, GO-Ag, and Ag/Zn-Ze were found in ascending order (Ag/Zn-Ze best). In addition, at 160 μg/mL concentration of Ag/Zn-Ze nanocomposite

Research Article
doi.org/10.1002/ansa.202100041
Chemistry Europe
European Chemical Societies Publishing

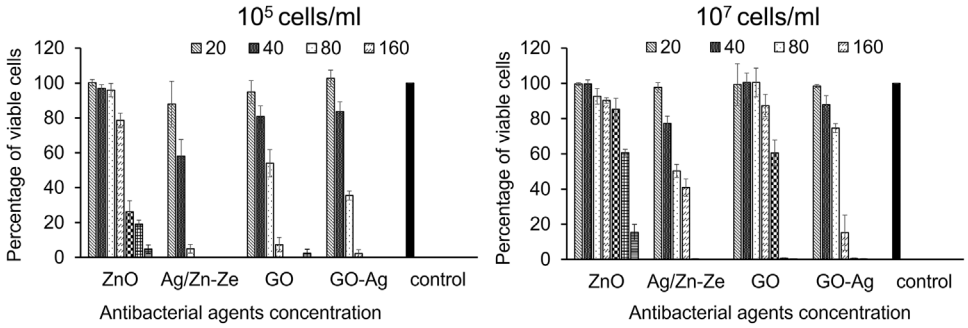

FIGURE 6 Percentage of viable *E. coli* cells for different dosage of antibacterial agents. Error bars indicate the standard error of three or more independent experiments

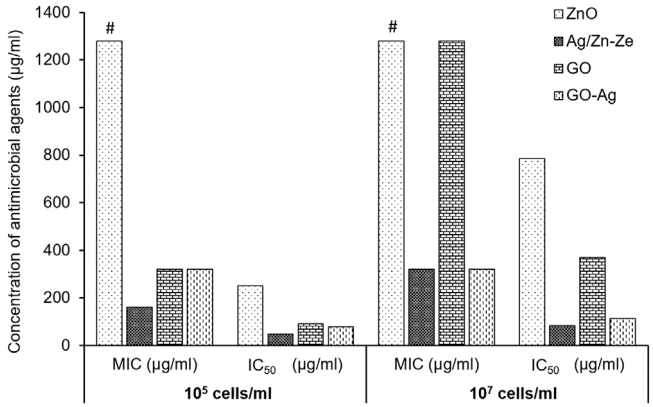

FIGURE 7 MIC and IC_{50} values for different antibacterial compounds. # indicates that MIC is greater than 1280 μg/mL

was able to remove 100% bacteria at lower initial bacterial concentration. Past studies show that for *E. coli*, the MICs of Ag and Zn-loaded zeolite are 32-64 μg/mL and 512-2048 μg/mL, respectively.[41] As it is known that composites have a synergistic effect in killing microorganisms, the prepared Ag/Zn-Ze nanocomposites exhibited noticeable antibacterial activities at a lower concentration than Ag-Ze and Zn-Ze both nanoparticles.

When the concentrations of antibacterial compounds are higher, ZnO fails to perform as good as the other compounds. Ag/Zn-Ze and GO-Ag exhibited better efficacy around the range of 320 to 640 μg/mL. Overall, Ag/Zn-Ze exhibited noticeably higher antibacterial efficacy compared to other compounds. In addition, from these findings, a clear dependence of the antibacterial efficacy on the initial bacterial concentration was clearly established. Figure 7 presents the summarized results of MIC and IC_{50}.

3.2.2 | Antimicrobial assay in plate culture

Table 1 and Figure S1 show the inhibition zone of ZnO nanoparticles, Ag/Zn-Ze nanocomposites, and GO-Ag nanocomposites. These nanomaterials showed quite good in zone of inhibition method. However, GO nanoparticles showed poor performance in plate culture. The reason is that GO does not diffuse through agar medium; as a result, its interaction with bacteria was less than other agents.

TABLE 1 Determination of inhibition capacity of ZnO, Ag/Zn-Ze, GO, and GO-Ag

Antibacterial agents' name	Mound diameter, mm	Average Inhibition diameter, mm	Inhibition thickness, mm
ZnO nanoparticles	6.8	11	2.1± 0.06
Ag/Zn-Ze nanocomposites	8.4	13	2.3± 0.03
GO nanoparticles	5.3	7.5	1.1± 0.06
GO-Ag nanocomposites	8.0	12.4	2.2± 0.10

In the case of ZnO nanoparticles, it has been reported that they exhibited inhibition zone thickness of 3 mm[42] at 1 mg/mL concentration and the inhibition zone thickness found from experiments was similar. However, no such study has been reported for Ag/Zn-Ze nanocomposites. The inhibition zone thicknesses of GO nanoparticles and GO-Ag nanocomposites were also reported to be 2 mm and 3 mm, respectively.[37]

3.3 | Antibacterial surface preparation

Based on the antibacterial efficacy test, Ag/Zn-Ze nanocomposites and GO-Ag nanocomposites were chosen for antibacterial surface preparation. These composites resisted the entrance of bacteria through the filter paper. Ag/Zn-Ze nanocomposites prevented around 50% of bacteria from entering the nutrient broth solution with respect to control. At this test, GO-Ag nanocomposites showed 97% prevention capacity with respect to control. The results of this experiment are presented in Table 2. The better performance of GO-Ag over Ag/Zn-Ze might be the higher binding of GO-Ag nanocomposites with filter paper during the physisorption process. At the time of experimenting, it was observed that the control solution was more turbid than the other two solutions whose openings were covered by antibacterial agent coated filter paper.

Research Article
doi.org/10.1002/ansa.202100041
Chemistry Europe
European Chemical Societies Publishing

TABLE 2 Bacterial prevention capacity of filter paper treated with Ag/Zn-Ze and GO-Ag nanocomposites

Antibacterial agents	Prevention capacity (%)
Ag/Zn-Ze nanocomposites	50 ± 11
GO-Ag nanocomposites	97± 3

3.4 | Cytotoxicity test

With the advance of medical science, nanomaterials are being used as a novel delivery system for proteins, DNA, RNA, and drugs.[43] However, different studies have proposed the working mechanism of antibacterial nanoparticles, by damaging the cell wall and hence destroying the cell's integrity.[44–47] This leads to the critical question about the toxicity of the nanoparticles towards mammalian cells. As nanoparticles are more toxic than large particles, knowing the toxicity before any potential application is extremely important. To assess the cytotoxicity of two nanocomposites, i.e., Ag/Zn-Ze and GO-Ag nanocomposites (which have performed better in antibacterial test), Vero, a healthy mammalian cell line was incubated in the presence of different concentrations of Ag/Zn-Ze and GO-Ag nanocomposites. Then cytotoxicity was measured after 24 h of incubation. Figure 8a indicates the highest number of viable cells for control, and it was also observed that a more significant number of viable cells was found for Ag/Zn-Ze than GO-Ag for each concentration. This indicates that Ag/Zn-Ze nanocomposites possess negligible cytotoxicity on Vero cells up to 500 μg/mL, whereas GO-Ag started to show its cytotoxicity from the beginning, and the percentage of viable cells gradually decreased with the increment of dosage.

From previous studies, it has been found that Ag/Zn-Ze nanocomposite has a cytotoxicity effect at 1000 μg/mL concentration on A549 alveolar adenocarcinoma cells.[48] As here, different type of cell line was used, the concentration of antibacterial compounds might be different to exhibit similar cytotoxicity. GO-Ag nanocomposite has been reported to have a cytotoxicity effect at a lower concentration of 5 μg/mL.[49]

Figure 8b and 8c compare the percentage of viable mammalian cells and viable bacterial cells incubated with different concentrations of Ag/Zn-Ze and GO-Ag nanocomposites, respectively. A plain solid line from Figure 8b confirms the mammalian nontoxicity behavior of Ag/Zn-Ze nanocomposites, maintaining a high antibacterial property against *Escherichia coli (E. coli.)*. On the contrary, for GO-Ag nanocomposites (Figure 8c) exhibited gradual downward curves for Vero cells and *E. coli.* cells with the increment of its concentration, which indicates the cytotoxic behavior of GO-Ag. However, IC_{50} for GO-Ag is 78 μg/mL, and the toxicity is not significant at that concentration. Furthermore, if this antibacterial compound is used externally, the cytotoxicity effect might be insignificant.

It is reported that nanoparticle cytotoxicity is heavily dependent on its shape and size.[50] Here, the spherical nanomaterials of sizes 18 and 25 nm have been studied. Previous studies showed that gold nanoparticles of 6 nm diameter are more toxic than 10 nm or larger nanoparticles.[51] *Zhao* et al. showed that needle and plate-shaped nanoparticles have higher toxicity than spherical and rod-shaped nanoparticles.[52] Considering the fact that these nanoparticles are larger than the reported size and possess negligible toxicity, they can be a potential candidate for in-vivo activity.

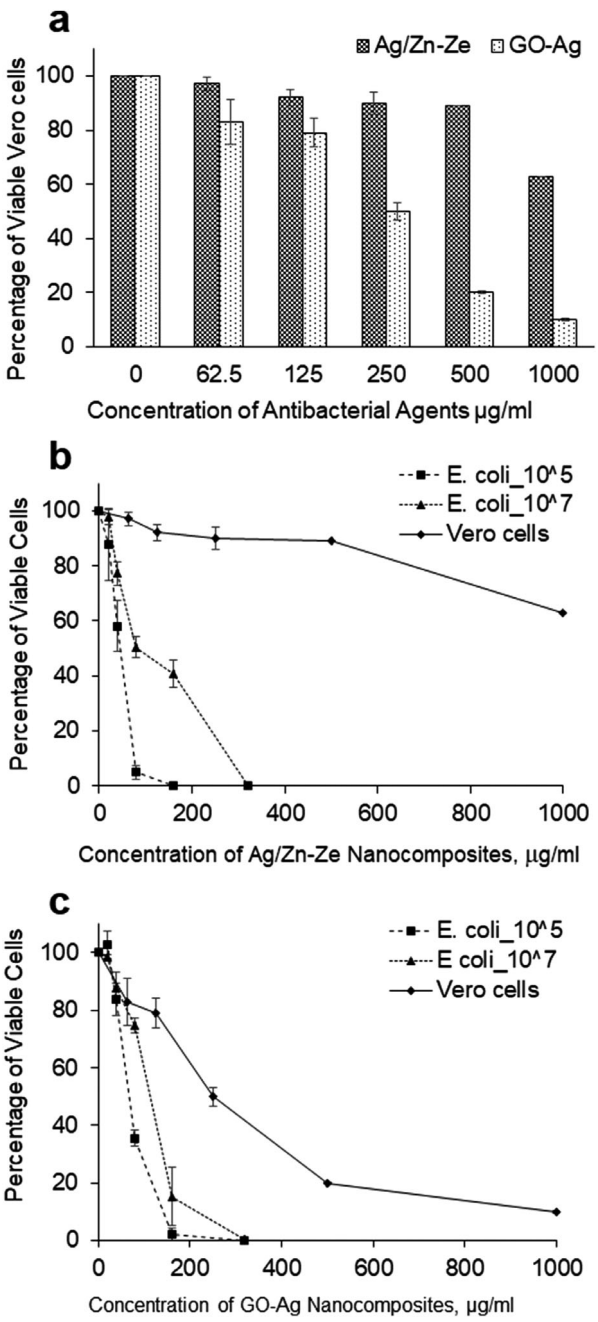

FIGURE 8 Observation of cytotoxicity of Ag/Zn-Ze and GO-Ag nanocomposites on mammalian cells (Vero cells) (a) Percentage of viable cells after incubation of 24 hrs with different concentrations of Ag/Zn-Ze and GO-Ag nanocomposites; (b-c) comparison of survival of mammalian cells (Vero) and bacterial cells (*E. coli.*) with different concentrations of Ag/Zn-Ze nanocomposites and GO-Ag nanocomposites. Error bars indicate the standard errors of multiple independent experiments

Research Article
doi.org/10.1002/ansa.202100041
Chemistry Europe
European Chemical Societies Publishing

4 | CONCLUSION

Antibacterial efficacy of the different concentrations of ZnO nanoparticles, Ag/Zn-Ze nanocomposites, GO nanoparticles, and GO-Ag nanocomposites were evaluated against *E. coli*. It is found that the antibacterial activities (MIC, IC_{50}) are highly dependent on initial bacterial concentrations. Ag/Zn-Ze nanocomposites and GO-Ag nanocomposites exhibited better antibacterial efficiency in solution. Their MICs were 160 μg/mL and 320 μg/mL for Ag/Zn-Ze and GO-Ag, respectively, for lower initial bacterial concentration. In the case of higher initial bacterial concentration, this was 320 μg/mL for both antibacterial agents. Performance of ZnO, Ag/Zn-Ze, and GO-Ag was nearly the same in the zone of inhibition test. However, GO exhibited poor efficacy compared to others. Interestingly, GO-Ag exhibited 97% prevention capacity when used in an antibacterial surface, whereas Ag/Zn-Ze efficacy was only 50%. However, Ag/Zn-Ze showed less cytotoxicity than GO-Ag when tested against healthy mammalian cells. This study established GO-Ag and Ag/Zn-Ze as two highly potent antimicrobial nanocomposites that can have varied applications, and the latter one is the most suitable one in case of any possible physiological interaction because of its non-hazardous characteristics.

ACKNOWLEDGMENT

The authors gratefully acknowledge the technical support from Applied Bioengineering Research incubator (ABRI), BUET.

DATA AVAILABILITY STATEMENT

The data that support the findings of this study are available from the corresponding author upon reasonable request.

CONFLICT OF INTEREST

The authors do not declare any conflict of interest.

ORCID

Shoeb Ahmed https://orcid.org/0000-0001-8215-5169

REFERENCES

1. Satcher D. Emerging infections: getting ahead of the curve. *Emerg Infect Dis*. 1995;1:1-6.
2. Kolár M, Urbánek K, Látal T. Antibiotic selective pressure and development of bacterial resistance. *Int J Antimicrob Agents*. 2001;17:357-363.
3. Morris JG Jr. How safe is our food?. *Emerg Infect Dis*. 2011;17:126.
4. Sawai J. Quantitative evaluation of antibacterial activities of metallic oxide powders (ZnO, MgO and CaO) by conductimetric assay. *J Microbiol Methods*. 2003;54:177-182.
5. Fu G, Vary PS, Lin C-T. Anatase TiO2 Nanocomposites for Antimicrobial Coatings. *J Phys Chem B*. 2005;109:8889-8898.
6. Hewitt C, Bellara S, Andreani A, Nebe-von-caron G, McFarlane C. An evaluation of the anti-bacterial action of ceramic powder slurries using multi-parameter flow cytometry. *Biotechnol Lett*. 2001;23:667-675.
7. Makhluf S, Dror R, Nitzan Y, Abramovich Y, Jelinek R, Gedanken A. Microwave-Assisted Synthesis of Nanocrystalline MgO and Its Use as a Bacteriocide. *Adv Funct Mater*. 2005;15:1708-1715.
8. Wang Y, Wan YZ, Dong XH, Cheng GX, Tao HM, Wen T. Preparation and characterization of antibacterial viscose-based activated carbon fiber supporting silver. *Carbon*. 1998;36:1567-1571.
9. Ma D, Xie C, Wang T, et al. Liquid-Phase Exfoliation and Functionalization of MoS2 Nanosheets for Effective Antibacterial Application. *ChemBioChem*. 2020;21:2373-2380.
10. Pelgrift RY, Friedman AJ. Nanotechnology as a therapeutic tool to combat microbial resistance. *Adv Drug Deliv Rev*. 2013;65:1803-1815.
11. Emerich DF. Nanomedicine–prospective therapeutic and diagnostic applications. *Expert Opin Biol Ther*. 2005;5:1-5.
12. Gajjar P, Pettee B, Britt DW, Huang W, Johnson WP, Anderson AJ. Antimicrobial activities of commercial nanoparticles against an environmental soil microbe, Pseudomonas putida KT2440. *Journal of Biological Engineering*. 2009;3:9.
13. Zhang L, Jiang Y, Ding Y, Povey M, York D. Investigation Into the Antibacterial Behaviour of Suspensions of ZnO Nanoparticles (ZnO Nanofluids). *J Nanopart Res*. 2007;9:479-489.
14. Rehman S, Asiri SM, Khan FA, et al. Biocompatible tin oxide nanoparticles: synthesis, antibacterial, anticandidal and cytotoxic activities. *ChemistrySelect*. 2019;4:4013-4017.
15. Chowdhury A-N, Azam MS, Aktaruzzaman M, Rahim A. Oxidative and antibacterial activity of Mn3O4. *J Hazard Mater*. 2009;172:1229-1235.
16. Akter N, Chowdhury L, Uddin J, Ullah AKMA, Shariare MH, Azam MS. N-halamine functionalization of polydopamine coated Fe3O4 nanoparticles for recyclable and magnetically separable antimicrobial materials. *Mater Res Express*. 2018;5:115007.
17. Islam MS, Akter N, Rahman MM, et al. Mussel-Inspired Immobilization of Silver Nanoparticles toward Antimicrobial Cellulose Paper. *ACS Sustainable Chemistry & Engineering*. 2018;6:9178-9188.
18. Boudghene-Guerriche A, Chaker H, Aissaoui M, et al. Evaluation of Antibacterial and Antioxidant Activities of Silver-Decorated TiO2 Nanoparticles. *ChemistrySelect*. 2020;5:11078-11084.
19. Chaudhary A, Kumar N, Kumar R, Salar RK. Antimicrobial activity of zinc oxide nanoparticles synthesized from Aloe vera peel extract. *SN Applied Sciences*. 2018;1:136.
20. Zhang L, Jiang Y, Ding Y, Povey M, York D. Investigation into the antibacterial behaviour of suspensions of ZnO nanoparticles (ZnO nanofluids). *J Nanopart Res*. 2007;9:479-489.
21. Suker DK, Albadran RM. Cytotoxic Effects of Titanium Dioxide Nanoparticles on Rat Embryo Fibroblast REF-3 Cell Line in vitro. *European J of Experimental Biology*. 2013;3(1):354-363.
22. Lanje A, Sharma S, Ningthoujam FNASR, Ahn JS, Pode R. Low temperature dielectric studies of zinc oxide (ZnO) nanoparticles prepared by precipitation method. *Adv Powder Technol*. 2013;24:331-335.
23. Doğan H, Koral M, İnan T. Ag/Zn Zeolite Containing Antibacterial Coating for Food-Packaging Substrates. *Journal of Plastic Film & Sheeting - J PLAST FILM SHEETING*. 2009;25:207-220.
24. Tetsuka H, Asahi R, Nagoya A, et al. Optically tunable amino-functionalized graphene quantum dots. *Advanced materials (Deerfield Beach, Fla)*. 2012;24:5333-5338.
25. Rasoulzadehzali M, Namazi H. Facile preparation of antibacterial chitosan/graphene oxide-Ag bio-nanocomposite hydrogel beads for controlled release of doxorubicin. *Int J Biol Macromol*. 2018;116:54-63.
26. Paulchamy B, Arthi G, Lignesh BD. A simple approach to stepwise synthesis of graphene oxide nanomaterial. *J Nanomed Nanotechnol*. 2015;6:1.
27. Kumar N, Srivastava VC. Simple synthesis of large graphene oxide sheets via electrochemical method coupled with oxidation process. *ACS omega*. 2018;3:10233-10242.
28. Islam MR, Ferdous M, Sujan MI, Mao X, Zeng H, Azam MS. Recyclable Ag-decorated highly carbonaceous magnetic nanocomposites for the removal of organic pollutants. *J Colloid Interface Sci*. 2020;562:52-62.
29. Shen J, Shi M, Li N, et al. Facile synthesis and application of Ag-chemically converted graphene nanocomposite. *Nano Res*. 2010;3:339-349.
30. Lanje AS, Sharma SJ, Ningthoujam RS, Ahn JS, Pode RB. Low temperature dielectric studies of zinc oxide (ZnO) nanoparticles prepared by precipitation method. *Adv Powder Technol*. 2013;24:331-335.

31. Shameli K, Ahmad MB, Zargar M, Yunus WMZW, Ibrahim NA. Fabrication of silver nanoparticles doped in the zeolite framework and antibacterial activity. *Int J Nanomed*. 2011;6:331.
32. Kumari S, Sharma P, Yadav S, et al. A Novel Synthesis of the Graphene Oxide-Silver (GO-Ag) Nanocomposite for Unique Physiochemical Applications. *ACS omega*. 2020;5:5041-5047.
33. Krishnamoorthy K, Umasuthan N, Mohan R, Lee J, Kim S-J. Antibacterial Activity of Graphene Oxide Nanosheets. *Sci Adv Mater*. 2012;4:1-7.
34. Chong JY, Wang B, Mattevi C, Li K. Dynamic microstructure of graphene oxide membranes and the permeation flux. *J Membr Sci*. 2018;549:385-392.
35. Rajaura RS, Srivastava S, Sharma V, et al. Role of interlayer spacing and functional group on the hydrogen storage properties of graphene oxide and reduced graphene oxide. *Int J Hydrogen Energy*. 2016;41:9454-9461.
36. Rokbani H, Daigle F, Ajji A. Combined Effect of Ultrasound Stimulations and Autoclaving on the Enhancement of Antibacterial Activity of ZnO and SiO_2/ZnO Nanoparticles. *Nanomaterials (Basel, Switzerland)*. 2018;8.
37. Sheet I, Holail H, Olama Z, Kabbani A, Hines M. The Antibacterial Activity of Graphite Oxide, Silver, Impregnated Graphite Oxide with Silver and Go-Coated Sand Nanoparticles Against Waterborne Pathogenic E. coli Bl21. *International Journal of Current Microbiology and Applied Sciences*. 2013;2:1-11.
38. Liu Y, He L, Mustapha A, Li H, Hu ZQ, Lin M. Antibacterial activities of zinc oxide nanoparticles against Escherichia coli O157:h7. *J Appl Microbiol*. 2009;107:1193-1201.
39. Chandraker K, Nagwanshi R, Jadhav SK, Ghosh KK, Satnami ML. Antibacterial properties of amino acid functionalized silver nanoparticles decorated on graphene oxide sheets. *Spectrochim Acta, Part A*. 2017;181:47-54.
40. Tang J, Chen Q, Xu L, et al. Graphene Oxide–Silver Nanocomposite As a Highly Effective Antibacterial Agent with Species-Specific Mechanisms. *ACS Appl Mater Interfaces*. 2013;5:3867-3874.
41. Demirci S, Ustaoğlu Z, Yılmazer GA, Sahin F, Baç N. Antimicrobial properties of zeolite-X and zeolite-A ion-exchanged with silver, copper, and zinc against a broad range of microorganisms. *Appl Biochem Biotechnol*. 2014;172:1652-1662.
42. Chaudhary A, Kumar N, Kumar R, Salar R. Antimicrobial activity of zinc oxide nanoparticles synthesized from Aloe vera peel extract. *SN Applied Sciences*. 2018;1.
43. Nowrouzi A, Meghrazi K, Golmohammadi T, et al. Cytotoxicity of Subtoxic AgNP in Human Hepatoma Cell Line (HepG2) after Long-Term Exposure. *Iranian biomedical journal*. 2010;14:23-32.
44. Liu C-C, Xu H, Wang L, Qin X. Facile One-Pot Green Synthesis and Antibacterial Activities of GO/Ag Nanocomposites. *Acta Metallurgica Sinica (English Letters)*. 2017;30:36-44.
45. Dutta P, Wang B. Zeolite-supported silver as antimicrobial agents. *Coord Chem Rev*. 2019;383:1-29.
46. Lu X, Feng X, Werber JR, et al. Enhanced antibacterial activity through the controlled alignment of graphene oxide nanosheets. *Proc Natl Acad Sci*. 2017;114:E9793.
47. Seil J, Webster T. Antimicrobial applications of nanotechnology: methods and literature. *Int J Nanomed*. 2012;7:2767-2781.
48. Samiei M, Ghasemi N, Aslaminabad N, Divband B, Golparvar-Dashti Y, Shirazi S. Zeolite-silver-zinc nanoparticles: biocompatibility and their effect on the compressive strength of mineral trioxide aggregate. *Journal of Clinical and Experimental Dentistry*. 2017;9.
49. Ali D, Alarifi S, Alkahtani S, Almeer RS. Silver-doped graphene oxide nanocomposite triggers cytotoxicity and apoptosis in human hepatic normal and carcinoma cells. *Int J Nanomedicine*. 2018;13:5685-5699.
50. Sukhanova A, Bozrova S, Sokolov P, Berestovoy M, Karaulov A, Nabiev I. Dependence of Nanoparticle Toxicity on Their Physical and Chemical Properties. *Nanoscale Res Lett*. 2018;13:44-44.
51. Huo S, Jin S, Ma X, et al. Ultrasmall gold nanoparticles as carriers for nucleus-based gene therapy due to size-dependent nuclear entry. *ACS nano*. 2014;8:5852-5862.
52. Zhao X, Ng S, Heng BC, et al. Cytotoxicity of hydroxyapatite nanoparticles is shape and cell dependent. *Arch Toxicol*. 2013;87:1037-1052.

SUPPORTING INFORMATION

Additional supporting information may be found in the online version of the article at the publisher's website.

How to cite this article: Hossain O, Rahman E, Roy H, Azam MdS, Ahmed S. Synthesis, characterization, and comparative assessment of antimicrobial properties and cytotoxicity of graphene-, silver-, and zinc-based nanomaterials. *Anal Sci Adv*. 2022;3:54–63. https://doi.org/10.1002/ansa.202100041